PHYSOR 2002, Seoul, Korea, October 7–10, 2002

CHANNEL BOWING EFFECTS ON PIN POWER DISTRIBUTIONS IN A WESTINGHOUSE SVEA-96+ ASSEMBLY

P. Grimm, F. Jatuff, A. Lüthi, M. Murphy, R. Seiler and R. van Geemert
Paul Scherrer Institute, Nuclear Energy and Safety Research Department
CH-5232 Villigen PSI, Switzerland
Peter.Grimm@psi.ch

T. Williams
Elektrizitäts-Gesellschaft Laufenburg AG
Lerzenstrasse 10, CH-8953 Dietikon, Switzerland
Tony.Williams@egl.ch

R. Chawla
Paul Scherrer Institute, CH-5232 Villigen PSI, Switzerland
and
Swiss Federal Institute of Technology, CH-1015 Lausanne, Switzerland
Rakesh.Chawla@psi.ch

Abstract

Effects of channel bowing on the pin power and ^{238}U capture rate distributions were studied experimentally and analytically in a test zone consisting of 9 full-size Westinghouse Atom SVEA-96+ fuel assemblies in the LWR-PROTEUS zero-power experimental facility. A very significant bowing was simulated by displacing the central test assembly by $\sim$9 mm in the two horizontal directions from its centered position in the 3×3 assemblies array. Calculations were performed for a whole-reactor model using the BOXER code and for a reflected assembly using CASMO-4. The agreement between calculated and measured reaction rate distributions in this configuration is of a similar quality as that in the case with the central assembly in its nominal position. The direct comparison of the measured and calculated effects of the displacement on the reaction rates (from two different LWR-PROTEUS configurations) confirms that the codes are capable of predicting this change with a high accuracy.

1 INTRODUCTION

One of the most important departures from nominal operating conditions in BWR cores is the mechanical deformation of fuel assembly channels (bending). This deformation during the irradiation of the fuel assemblies in the reactor, commonly referred to as channel bowing, is mainly due to variations of the fast neutron fluence between the different sides of the assembly. Typically, the wall of the channel adjacent to a control blade is irradiated less than that on the opposite side. From the point of view of lattice physics, channel bowing expresses itself as a change of the widths of the inter-assembly water gaps (typically smaller than nominal on one assembly side and larger on the opposite side). This change affects the neutron moderation conditions particularly for peripheral and corner pins, which in turn influence the neutron spectrum and the power in these pins, and the response of nearby instrumentation. Channel

bowing effects introduce additional uncertainties in the prediction of local power distributions and maximum linear heat generation rate that can impose a penalty of typically $\sim$6% to the maximum reactor power. A precise characterization of channel bowing effects is thus important with regard to operational limits of BWR's. The purpose of the current paper is to describe the first-of-its-kind experimental validation of channel bowing effects for modern 10 $\times$ 10 BWR fuel undertaken in LWR-PROTEUS.

2 THE LWR-PROTEUS PHASE I EXPERIMENTS

One of the most significant, recent experimental programmes in reactor physics for code validation of modern LWR fuel assemblies is the LWR-PROTEUS project, a co-operation between the Swiss Nuclear Utilities and the Paul Scherrer Institute in Switzerland [1]. The goal of LWR-PROTEUS Phase I has been the validation of neutron transport codes like CASMO-4, HELIOS, BOXER, PHOENIX and MCNP in the estimation of reactor physics parameters such as rod-by-rod reaction rate distributions and reactivity effects that have been measured in an actual Westinghouse SVEA-96+ assembly. The purpose of using actual fuel assemblies is to gain realism and to address specific uncertainties, such as tolerances and departures from nominal conditions, during the validation process itself.

The LWR-PROTEUS reactor configuration is essentially a coupled system, consisting of a central test region of LWR fuel elements driven critical by annular thermal driver zones. The facility was configured to provide an appropriate LWR neutron spectrum environment to a centrally-located SVEA-96+ fuel assembly in which measurements are carried out (the *test element*). The test element is surrounded by 8 other identical assemblies (see Fig. 1), the 3 $\times$ 3 arrangement (the *test zone*) being located inside an aluminium test tank. Since the elements are 4.5 m in length and the active height of the PROTEUS driver regions is about 1 m, the test tank can be moved axially to enable step-wise investigations along the whole length of the test assemblies. The test zone is surrounded by outer radial regions (the buffer, the D2O-driver, the graphite-driver and a graphite reflector) which govern the criticality of the reactor, thus allowing experiments for a wide range of test lattices. A SVEA-96+ fuel assembly comprises 96 fuel rods arranged in four separate subbundles, each containing 24 rods on a square pitch around a central water canal (see Fig. 1). The ^{235}U enrichment varies both axially and radially in the range 2–5% and some rods contain, additionally, gadolinia as an integral burnable absorber.

The measurements have covered the most important features of the SVEA-96+ design, namely:

- Assembly radial heterogeneities: Geometrically-complex by-pass regions, relatively large number of burnable absorber fuel rods, heterogeneous ^{235}U-enrichment distribution, etc.
- Assembly axial heterogeneities: Axial regions with different average ^{235}U-enrichment and materials distributions, spacers, some studies on part-length rods, etc.
- Core heterogeneities: Presence of fully- and partly-inserted absorber blades, channel bowing, and their effect on instrumentation response.

Experiments were performed for full-density water moderation and for simulated partial voiding (using plastic inserts in a dry test zone). The results of investigations related to the inherent assembly heterogeneities have been published recently [2, 3].

3 MEASUREMENTS FOR CHANNEL BOWING EFFECTS

Channel bowing was simulated in LWR-PROTEUS by displacing the central test assembly from its regular position in the test zone arrangement by approximately 9 mm in the two horizontal directions, as shown in Figure 1. Special upper and lower grids were used in this configuration, which is called LWR-PROTEUS core 7A. The displacement means that the nominal inter-assembly gaps (13.8 mm on all 4 sides) were changed to two narrow gaps of $\sim$5 mm on the south and east sides and two wide gaps of $\sim$23 mm at the north and west sides. This rather large bowing was selected in order to emphasize the moderation condition changes, thus constituting an upper bound (typical bowings involve departures from the nominal gap of 2–3 mm). It also assures a well-measurable effect that clearly exceeds uncertainties coming from the measurements (such as counting statistics) or possible deviations of the assembly geometry from nominal dimensions. The investigations were performed for the lower part of the SVEA-96+ assemblies (average ^{235}U enrichment of 4.02%) under full-density water moderation. The comparison of data measured in this configuration with those obtained previously for the test element centered in the test zone (core 1A, see [3]) allows a direct experimental assessment of the effects of channel bowing.

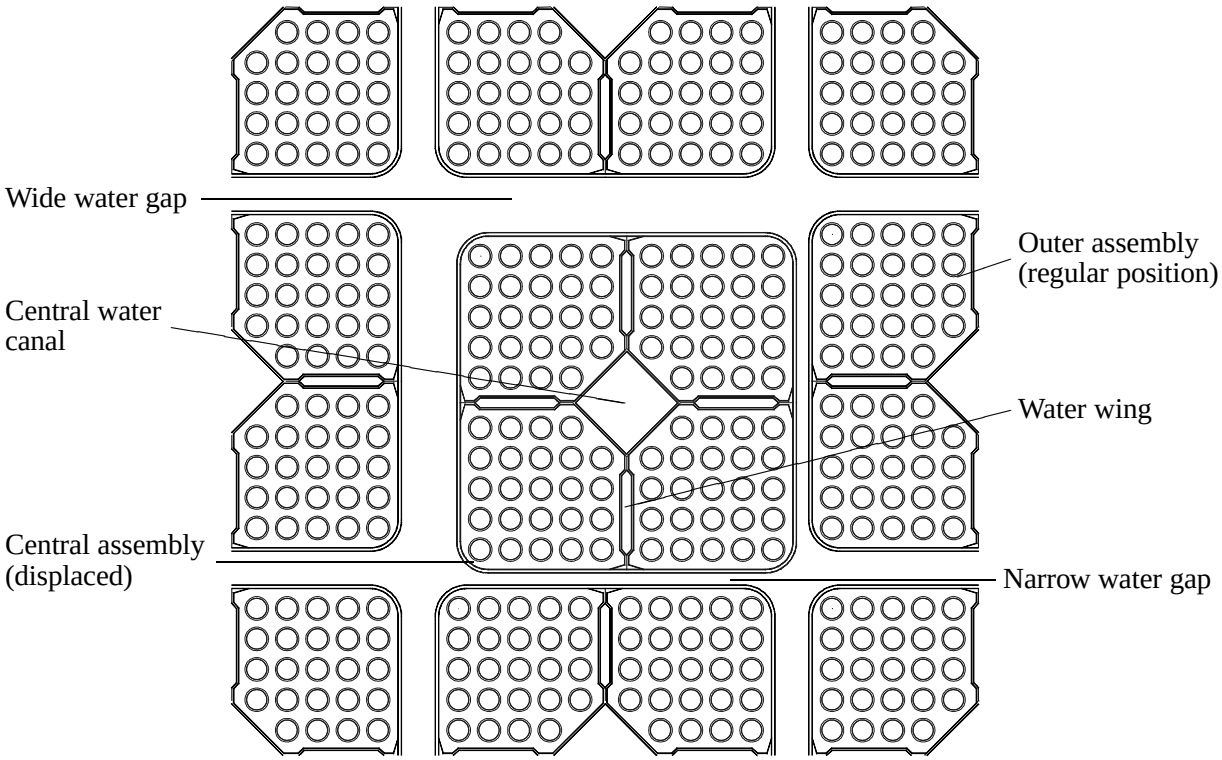

Figure 1: LWR-PROTEUS core 7A test zone with a displaced central SVEA-96+ assembly and 8 surrounding assemblies in regular arrangement (only parts adjacent to central assembly shown).

The distributions of the total fission rate (F_{tot}) and of the ^{238}U capture rate (C_8) were determined by γ-ray scanning of 64 different fuel pins (out of a total number of 96). After 1 hour of irradiation at a reactor power of 30 watts, the selected pins (10 per batch) were transferred to the automatic γ-scanner and counted repeatedly (one pin at a time) during about 18 hours. The γ-ray spectra were measured using two horizontally opposed germanium detectors. From these spectra, γ lines of four fission product

nuclides (with suitable half-lives, intensities and separation from interfering lines) and one of ^{239}Np (for the C_8 distribution) were identified, the background continuum subtracted, peak areas deconvoluted, and processed into maps of relative reaction rates per pin.

The statistical uncertainties of the reaction rate distributions were derived from the conventional analysis of count rates, detector dead-times, etc., as also from the averaging of results from the different photopeaks used for obtaining the F_{tot} distributions. The average 1σ statistical errors associated with gamma-ray counting were 0.48% for F_{tot} and 0.54% for C_8, with values for individual pins in the ranges 0.36 to 0.96% and 0.41 to 1.22%, respectively.

The fuel rod arrangement in the SVEA-96+ element is symmetric with respect to the northwest–southeast diagonal. Ratios of reaction rates measured for symmetrical positions are thus expected to be very close to unity. The diagonal symmetries obtained in the current measurements were indeed very good, the mean of the ratios obtained for the 21 different pairs of corresponding fuel rods being 0.9998 and 0.9948 for F_{tot} and C_8, respectively. The standard deviations of the ratios for an individual pin pair for the two reaction rates are 1.0 and 0.7%, and are thus comparable to those to be expected from the statistical uncertainties on the individual pin values.

4 CODES AND MODELS USED FOR THE CALCULATIONS

Calculations were performed using the CASMO-4 [4] and BOXER [5] codes. CASMO-4 is a well-known fuel assembly neutronics code developed by Studsvik Scandpower Inc. An important feature of CASMO-4 is the characteristics method used for the solution of the transport equation in two dimensions, which allows an explicit modelling of the fuel pins without cell homogenization. However, its capabilities are limited to the calculation of single assemblies with reflective boundary conditions. CASMO-4 version 1.28.05H and the J2LIB cross-section library, based on JEF-2.2 nuclear data, were used for the present calculations. BOXER is a lattice code developed at PSI. It performs cell and two-dimensional transport and depletion calculations in Cartesian geometry. The cell calculations are performed using a point-wise calculation for resonance self-shielding (between 1.3 and 907 eV) and a one-dimensional integral transport calculation in cylindrical geometry for the group-wise calculation. The two-dimensional transport calculations are performed by means of a transmission probability integral transport method in x-y geometry for homogenized cells, using first-order spherical harmonics expansions for the mesh surface currents and a linear space dependence for surface currents and the source within the meshes.

In all the calculations, care was taken to model the actual geometry of the test zone as accurately as possible. In particular, values measured in the PROTEUS core configuration were used for the gaps between the central test element and its four neighbours (they are not perfectly symmetric relative to the diagonal) and for the position of the pins within the assembly. The enrichments of the fuel pins used in the calculations were measured values reported in the fuel manufacturer's quality control documentation.

The reaction rate distributions from BOXER were obtained using an x-y model of a horizontal section through the whole PROTEUS reactor, in which each pin cell in the test zone was represented explicitly. A refined and somewhat irregular mesh grid had to be used to represent the cell boundaries both in the displaced central element and in the outer 8 assemblies. The model for the outer zones of the reactor was simplified, in particular the circular zone boundaries were replaced by square boundaries enclosing the same cross-sectional area. The actual as-built critical configuration of core 7A was modelled, but with the driver loading reduced for the estimated equivalent of absorbing structures not included in

the model. The axial buckling was adjusted manually so as to achieve the critical condition (k_{eff} = 1). 24 energy groups were used for the two-dimensional transport calculations. This structure was optimized for the PROTEUS whole-reactor model and comprises a rather large number of groups in the high (E $>$ 300 keV) and thermal energy ranges.

CASMO-4 calculations were carried out for the central test assembly with reflective boundary conditions. The boundaries were placed in the middle of the water gaps between this assembly and its four nearest neighbours. The calculations were performed in a manner representative of routine production calculations using default options and standard modelling. Due to the slight asymmetry of the inter-assembly water gaps, the full assembly had to be calculated, without diagonal symmetry. The resulting reaction rate distributions were converted to the actual PROTEUS situation using so-called single zone correction factors. These corrections were computed as the ratios of the respective quantities from the whole-reactor and reflected-assembly BOXER calculations. The same mesh grid was used in the latter two calculations in order to obtain correction factors which are practically free from numerical effects. The corrections are relatively substantial at the corners, particularly at the corner facing the two narrow water gaps, where the correction for F_{tot} reaches +12%. This is due to the fact that the reflected-assembly model implicitly assumes the gaps between the neighbouring assemblies to be also reduced and hence underestimates the quantity of water influencing this corner (cf. Fig. 1). The opposite happens at the other three corners, i.e. the corrections are negative, but smaller in absolute magnitude than the above value. In the interior of the assembly, the corrections amount only to a few percent and vary smoothly, representing the global radial flux curvature in the finite test zone. The comparison of the reflected-assembly results obtained using CASMO-4 with experimental data has to rely relatively strongly on the single zone correction factors from BOXER. However, possible deviations of the BOXER results from the truth would affect both the reflected-assembly and whole-reactor calculations in a similar manner, so that the quality of these factors can be expected to be better than that of the results for the individual models.

5 COMPARISON OF CALCULATED AND MEASURED VALUES

Both measured (E) and calculated (C) pin-by-pin distributions were first normalized to the same average value for the 64 measured pins. The thus normalized C and E values were then compared in terms of C/E ratios for the total fission rate and the ^{238}U capture rate in each measured pin. In these comparisons, it should be borne in mind that the experimental statistical uncertainties (1σ) are typically 0.5% for both F_{tot} and C_8.

When studying the deviations of the calculated values from the experiment, it is also interesting to compare them to the changes of the reaction rates due to the displacement of the central assembly (between cores 1A and 7A). Peripheral pins adjacent to the wide water gaps have higher values for both F_{tot} and C_8 in the case of the displaced element and lower values are found for pins near the narrow gaps. The maximum changes due to the large displacement of 9 mm are approximately 16% for F_{tot} and 6% for C_8 and can typically be found in peripheral pins near the middle of the sides of the assembly. Although one might expect intuitively the largest changes in the corner pins, it is quite obvious that the latter pins experience a less drastic change in moderation than those in the middle of the sides (for example, the narrow-narrow corner pin is influenced by a relatively large quantity of water in the unchanged gaps between the neighbouring assemblies, cf. Fig. 1).

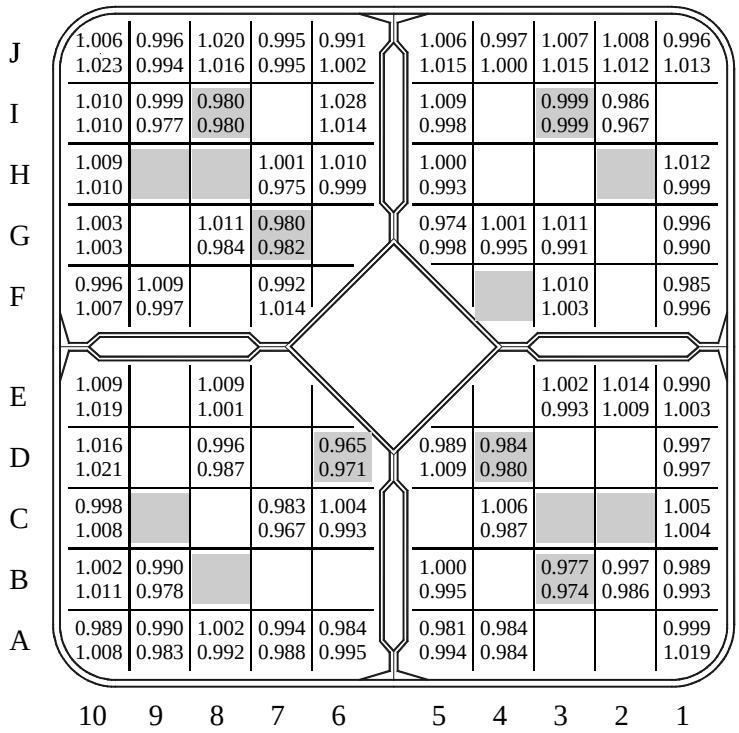

Figure 2: C/E ratios for the total fission rate as obtained with CASMO-4 (upper values) and BOXER (lower values). Shaded squares represent Gd-poisoned pins.

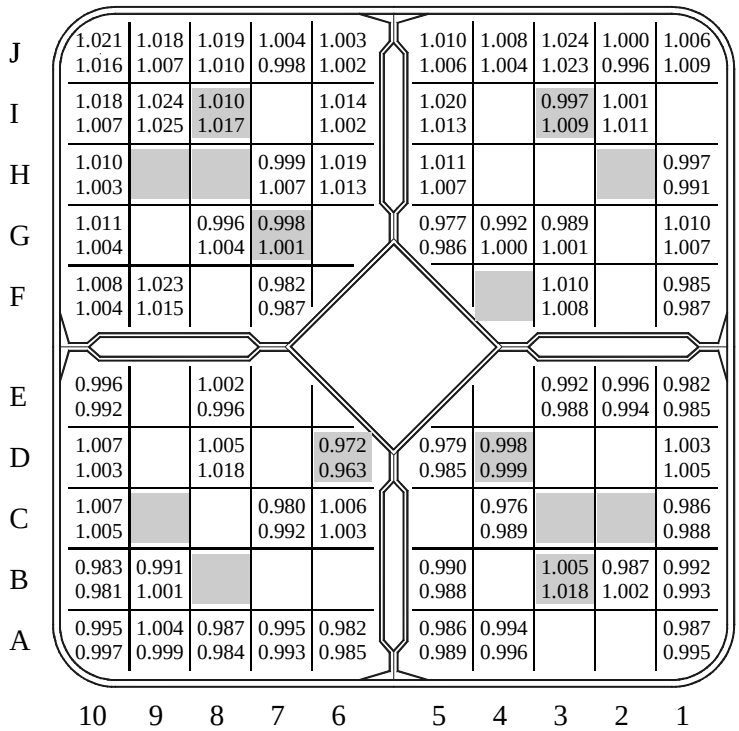

Figure 3: C/E ratios for the ^{238}U capture rate as obtained with CASMO-4 (upper values) and BOXER (lower values). Shaded squares represent Gd-poisoned pins.

Table I: Statistics of the C/E deviations

Reaction	Code	RMS (%)	Maximum	Minimum
F_{tot}	CASMO-4	1.2	1.028	0.965
	BOXER	1.4	1.023	0.967
C_8	CASMO-4	1.3	1.024	0.972
	BOXER	1.1	1.025	0.963

The distributions of C/E ratios are shown in Figure 2 for F_{tot} and in Figure 3 for C_8. The root-mean-square of the C/E deviations and the maximum and minimum values (i.e. the largest deviations from unity) are shown in Table I. The results generally indicate a good agreement between the calculated and measured values. The RMS, maximum and minimum deviations are comparable to those observed previously for other LWR-PROTEUS experiments [2, 3]. The agreement of the BOXER results with the measured data is actually better than that for regular inter-assembly gaps [3], whereas the deviations of the CASMO-4 results are slightly larger. In the case of BOXER, this appears to be due to the refined mesh grid imposed by the superposition of cell boundaries in the regular and displaced assembly positions in the core 7A model. This refinement of the meshes actually tends to mitigate some of the systematic deviations of BOXER results from the experiment.

Some trends can be observed in Figures 2 and 3. The most conspicuous deviation is a systematic underprediction of the total fission rate in the Gd-poisoned pins by $\sim$2% on the average in both codes. BOXER tends to overpredict somewhat F_{tot} of the corner pins and to underpredict that of UO_2 pins with two burnable absorber (BA) neighbours, such as pins I2, C7 and H7. For the ^{238}U capture rate a concentration of slightly high C/E ratios can be seen in the peripheral pins adjacent to the wide water gaps (row J and column 10) both for CASMO-4 and BOXER, whereas low values are found in the pins surrounding the central water canal. There is no systematic trend for C_8 in the BA pins. These trends are typical for the two codes and have also been observed for the case with the central test element in its regular position [3].

F_{tot}

CASMO-4	
1.002	1.000
0.996	0.995

BOXER	
0.999	0.999
0.995	0.995

C_8

CASMO-4	
1.010	1.002
0.994	0.990

BOXER	
1.007	1.004
0.994	0.994

Figure 4: Average C/E ratios per subbundle

In this configuration with a displaced central assembly it is of particular interest to check for spatial trends of the C/E ratios in the direction of the displacement, i.e. diagonally from northwest to southeast. To facilitate this investigation, average C/E values have been computed for each of the four subbundles. They are shown in Figure 4. The results show that there is a slight tilt for both reactions and both codes with higher average C/E in the northwest subbundle (adjacent to the two wide gaps) than in the southeast (near the narrow gaps). The trend is more pronounced for C_8 than for F_{tot} and more with CASMO-4 than with BOXER. The differences between subbundle averages are in all the cases larger than what could be expected from the experimental statistical uncertainties (for these averages, they are about 1/4 of the values for a single pin, i.e. in the range 0.10 to 0.15%). However, a less significant trend can also be observed in the other diagonal direction (northeast–southwest), which cannot be currently explained.

The capabilities of the lattice codes in predicting the effects of the displacement of the central assembly (or of channel bowing) can be assessed directly by comparing the results for cores 1A (test element centered, see Ref. [3]) and 7A (test element displaced). For this purpose, ratios of the measured and calculated reaction rates between the two configurations were determined for those pins investigated in both cases (a few more pins were measured in core 7A than in core 1A), each of the reaction rate distributions being renormalized to an average of unity in this common subset. For this comparison, the BOXER values for core 1A were taken from a calculation for a reflected assembly in which each pin cell was evenly divided into 2×2 meshes, and corrected for the global flux curvature in the LWR-PROTEUS test zone by multiplying with the ratios of BOXER results from the whole-reactor and reflected-assembly models (with 1 mesh per pin cell). This was done in order to get a fair comparison with the core 7A results, not affected by numerical effects of the mesh widths (in test calculations, effects of mesh refinement up to $\sim$1.5% on the F_{tot} distribution were found, whereas the differences between 2×2 meshes per pin cell and the grid used for core 7A are negligible). The BOXER results used for core 1A in the present study are therefore different from those used in Ref. [3]. The CASMO-4 results were converted to the actual LWR-PROTEUS situation using the appropriate correction factors from BOXER calculations for each of the cores. C/E ratios for the change of the reaction rates between the two configurations (or for the effect of channel bowing) were computed in the same way as shown above for the reaction rates. These C/E ratios for F_{tot} and C_8 are shown in Figures 5 and 6, respectively. The statistical uncertainties of the measured ratios are determined by the combination of the errors of the two measurements and amount to typically 0.7% for F_{tot} and 0.9% for C_8.

Generally, Figures 5 and 6 show that the two codes predict the impact of channel bowing on the reaction rate distributions with good accuracy. The RMS C/E deviations are 1.1% and 1.7% for the effects on F_{tot} and C_8, respectively, with CASMO-4, and 1.2% and 1.4% in the case of BOXER calculations. They are only slightly larger than the uncertainties of the measured values, particularly for F_{tot}. The C/E ratios for both reactions and both codes in the pins near the wide-wide corner (northwest) are mostly greater than 1 and those near the narrow-narrow corner (southeast) less than unity. This suggests that the calculations tend to exaggerate somewhat the effect of channel bowing. This trend seems to be more pronounced for C_8 than for F_{tot} and more with CASMO-4 than with BOXER. As for the C/E values in the case of the displaced test assembly (see above), a slight tilt in the other diagonal direction can also be noted (there are more C/E ratios greater than 1 in the northeast subbundle than in the southwest).

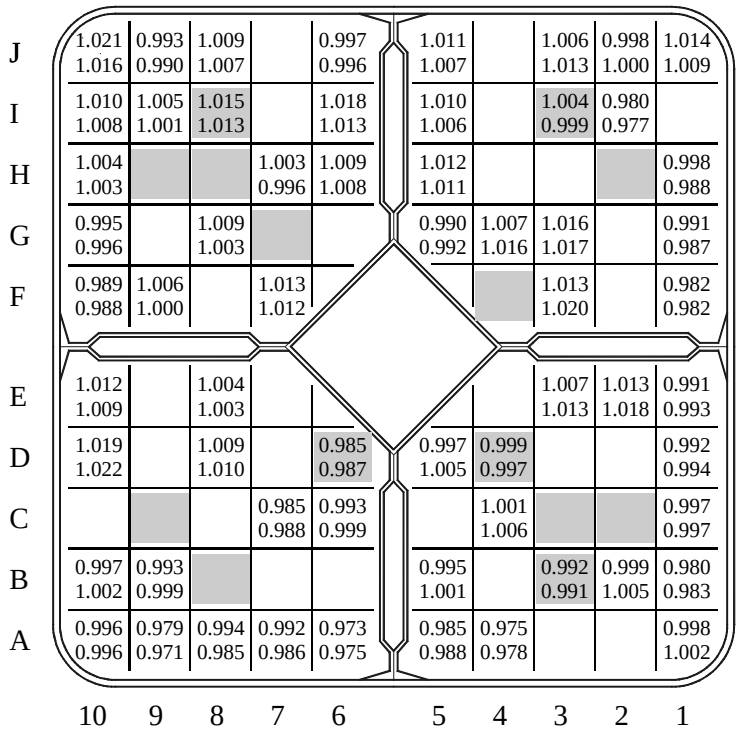

Figure 5: C/E ratios for the effect of channel bowing on F_{tot} as obtained with CASMO-4 (upper values) and BOXER (lower values). Shaded squares represent Gd-poisoned pins.

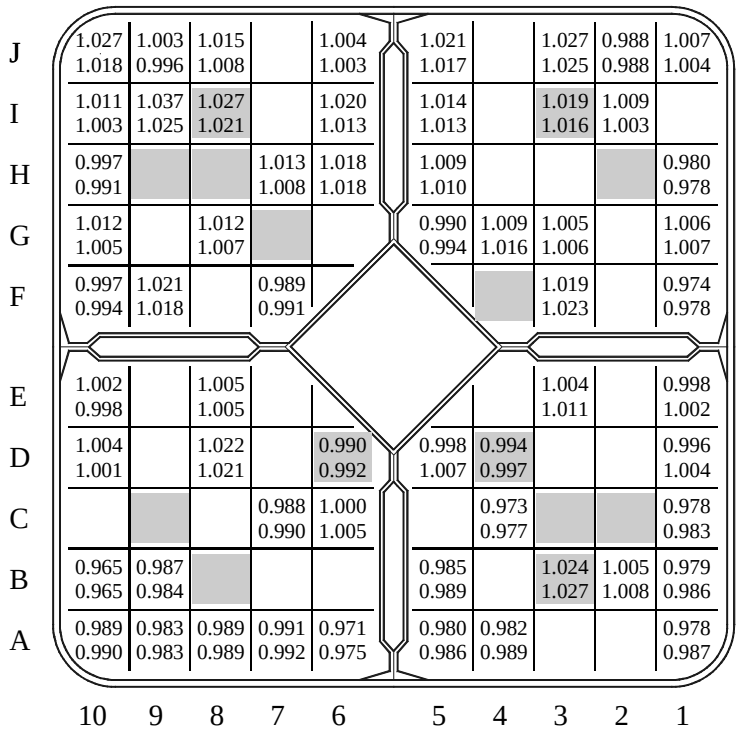

Figure 6: C/E ratios for the effect of channel bowing on C_8 as obtained with CASMO-4 (upper values) and BOXER (lower values). Shaded squares represent Gd-poisoned pins.

6 CONCLUSIONS

Channel bowing effects on the total fission and ^{238}U capture rate distributions have been studied experimentally and analytically in the framework of the LWR-PROTEUS Phase I project. A very significant bowing ($\sim$9 mm) has been simulated by displacing the central test assembly from its nominal position in a test zone of 9 Westinghouse Atom SVEA-96+ fuel assemblies under full-density water moderation. This rather large bowing was selected in order to produce a significant effect exceeding experimental uncertainties.

The calculations performed using the CASMO-4 and BOXER codes show that the effect of channel bowing on the pin power and ^{238}U capture distributions is quite predictable. The quality of the C/E comparisons is not inferior to the cases where the central assembly was placed in a nominally regular arrangement. A comparison between LWR-PROTEUS cores 1A and 7A, i.e. with the central assembly in the two positions, also shows that the changes of these reaction rates due to the displacement of the assembly are well predicted. These findings, together with geometrical data on channel bowing in operating cores, could possibly lead to a reduction of corresponding penalties imposed on the maximum reactor power.

ACKNOWLEDGEMENTS

The LWR-PROTEUS Phase I programme has been conducted jointly by PSI and the Swiss Nuclear Utilities (UAK) with specific contributions from Elektrizitäts-Gesellschaft Laufenburg (EGL). We are particularly grateful to the UAK representatives H. Achermann, H. Fuchs, D. Furtado, G. Meier, R. Stratton, G. Straub, as also R. Brogli and W. Kröger (PSI), S. Helmersson (Westinghouse Atom) and W. Färber (ex-EGL) for their strong support of the experiments. Also thanked are P. Bourquin, M. Berweger and R. Winter for excellent reactor operation and maintenance, as well as J. Ulrich, G. Von Holzen and K. Kohlik of PSI's Logistics and Marketing Department (LOG) for their valuable engineering support.

References

[1] T. Williams, R. Chawla, P. Grimm, O.P. Joneja, R. Seiler, A.K. Ziver, "LWR-PROTEUS — New Experiments at a Zero-Power Facility Using Power Reactor Fuel," *Proc. Int. Conf. on the Physics of Nuclear Science and Technology,* Long Island, NY, Oct. 5–8, 1998, Vol. 1, pp. 720–727

[2] F. Jatuff, P. Grimm, O. Joneja, M. Murphy, A. Lüthi, R. Seiler, R. Brogli, R. Jacot-Guillarmod, T. Williams, S. Helmersson, R. Chawla, "LWR-PROTEUS Verification of Reaction Rate Distributions in Modern 10 x 10 Boiling Water Reactor Fuel," *Nucl. Sci. Eng.*, **139**, pp. 262–272 (2001)

[3] M. Murphy, A. Lüthi, R. Seiler, P. Grimm, O. Joneja, A. Meister, R. van Geemert, F. Jatuff, R. Brogli, R. Jacot-Guillarmod, T. Williams, S. Helmersson, R. Chawla, "Neutronics Investigations for the Lower Part of a Westinghouse SVEA-96+ Assembly," *Nucl. Sci. Eng.*, **141**, pp. 32–45 (2002)

[4] D. Knott, B. Forssén, M. Edenius, "CASMO-4, A Fuel Assembly Burnup Program: Methodology," SOA-95/2, Studsvik of America (1995)

[5] J.M. Paratte, K. Foskolos, P. Grimm, J.M. Hollard, "ELCOS, The PSI Code System for LWR Core Analysis. Part II: User's Manual for the Fuel Assembly Code BOXER," PSI Bericht Nr. 96-08, Paul Scherrer Institute (1996)